

Figure S1. Validation of some miR-26b and miR-98 HOCTAR predicted targets by dual luciferase assays. 3' UTRs of the analyzed genes were cloned into a firefly luciferase sensor construct and transfected into HeLa cells along with a Renilla Luciferase control. The luciferase activity was measured in the presence or in the absence of plasmid constructs containing the precursor sequences of hsa-miR-26b (left 4 genes) and hsa-miR-98 (right 7 genes). The gene CTSA and MTDH, which were not predicted targets of miR-26b and miR-98, respectively, were used as negative controls. These results were highly correlated to the results detected by qRT-PCR in the experiments described in Fig. 3A and Fig. 3B.

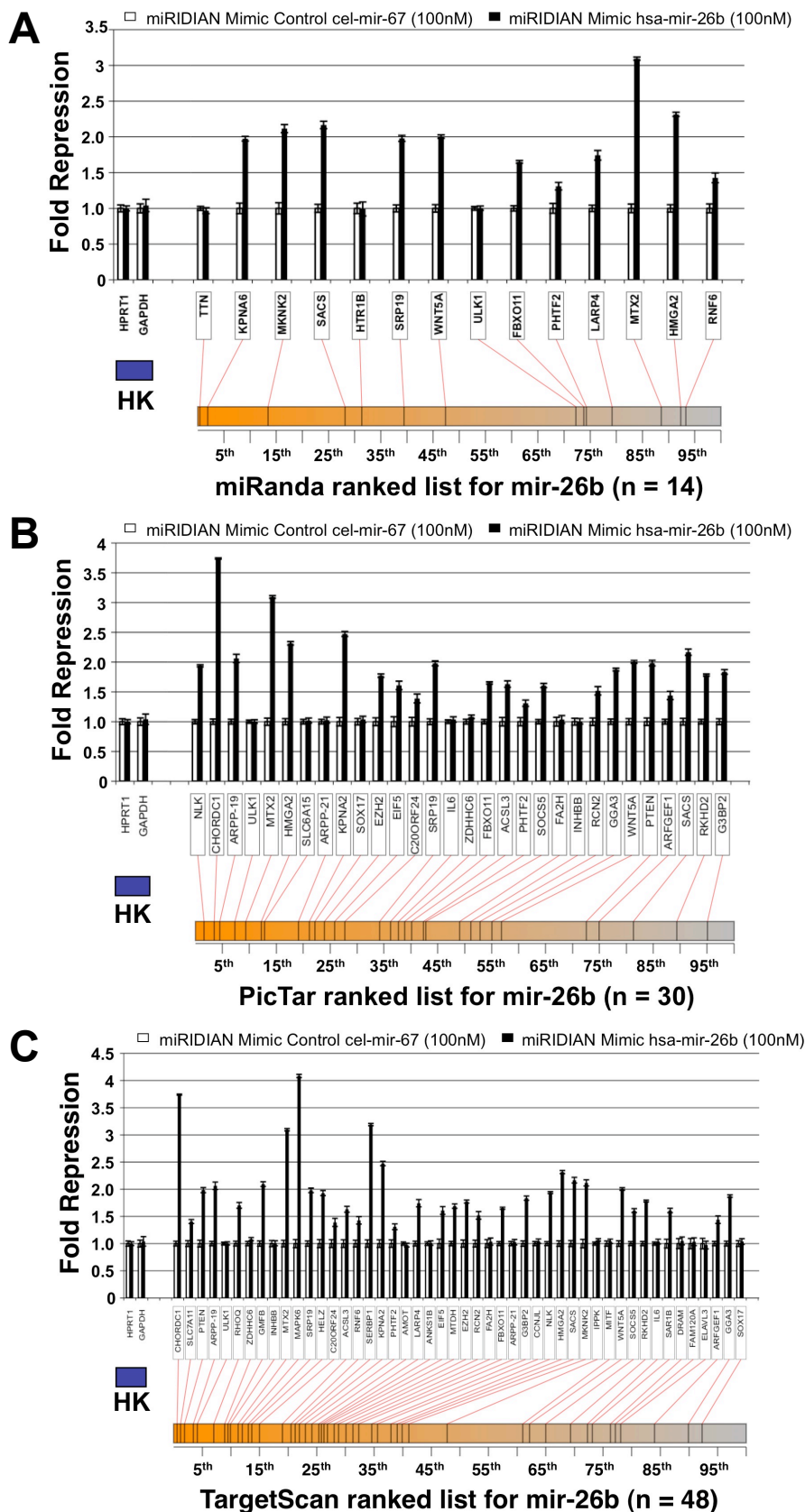


Figure S2. Distribution of the genes analyzed after overexpression of mimic-miR-26b in HeLa cells, as reported in Figure 3A, within the ranked lists of TargetScan, PicTar and miRanda for miR-26b. The histograms show the differences in the expression levels between miRNA-overexpressed HeLa cells (black bars) and control (cel-miR-67 transfected) HeLa cells (white bars), of a subset of miRanda (panel A), PicTar (panel B) and TargetScan (panel C) predicted target genes for miR-26b. Y-axis: fold change repression (expressed as $2^{-\Delta\Delta C_t}$ values). X-axis: predicted target genes tested (their symbols are indicated in the boxes). The target genes tested were homogeneously distributed along the entire ranked lists pertaining to each of these prediction softwares and the red lines below the diagrams indicate the ranking of each target genes tested within miRanda (A), PicTar (B) and TargetScan (C) prediction lists for miR-26b. The HK indicate the house-keeping genes used to normalize the expression levels.

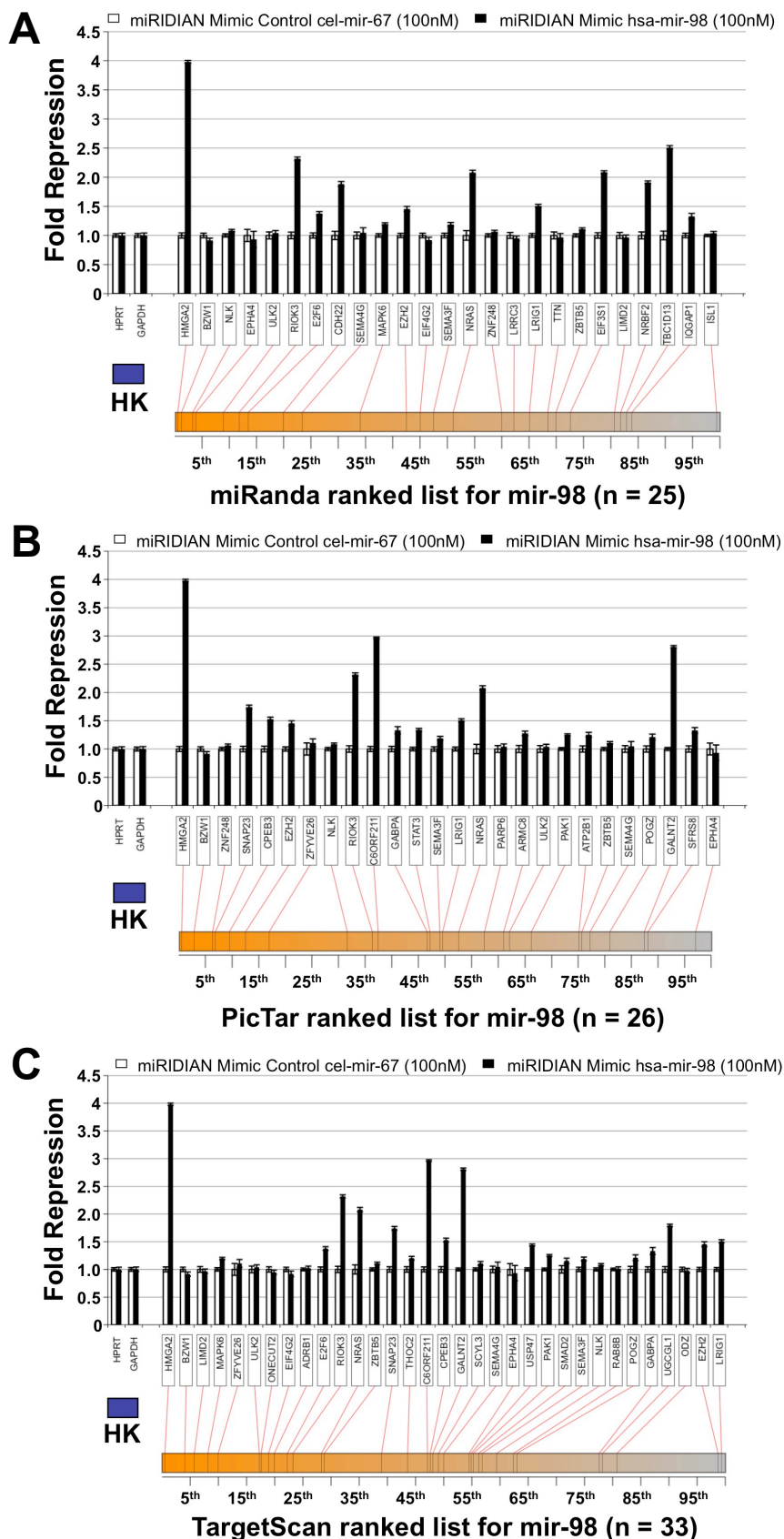


Figure S3. Distribution of the genes analyzed after overexpression of mimic-miR-98 in HeLa cells, as reported in Figure 3B, within the ranked lists of TargetScan, PicTar and miRanda for miR-98. The histograms show the differences in the expression levels between miRNA-overexpressed HeLa cells (black bars) and control (cel-miR-67 transfected) HeLa cells (white bars), of a subset of miRanda (panel A), PicTar (panel B) and TargetScan (panel C) predicted target genes for miR-98. Y-axis: fold change repression (expressed as $2^{-\Delta\Delta C_t}$ values). X-axis: predicted target genes tested (their symbols are indicated in the boxes). The target genes tested were homogeneously distributed along the entire ranked lists pertaining to each of these prediction softwares and the red lines below the diagrams indicate the ranking of each target genes tested within miRanda (A), PicTar (B) and TargetScan (C) prediction lists for miR-98. The HK indicate the house-keeping genes used to normalize the expression levels.

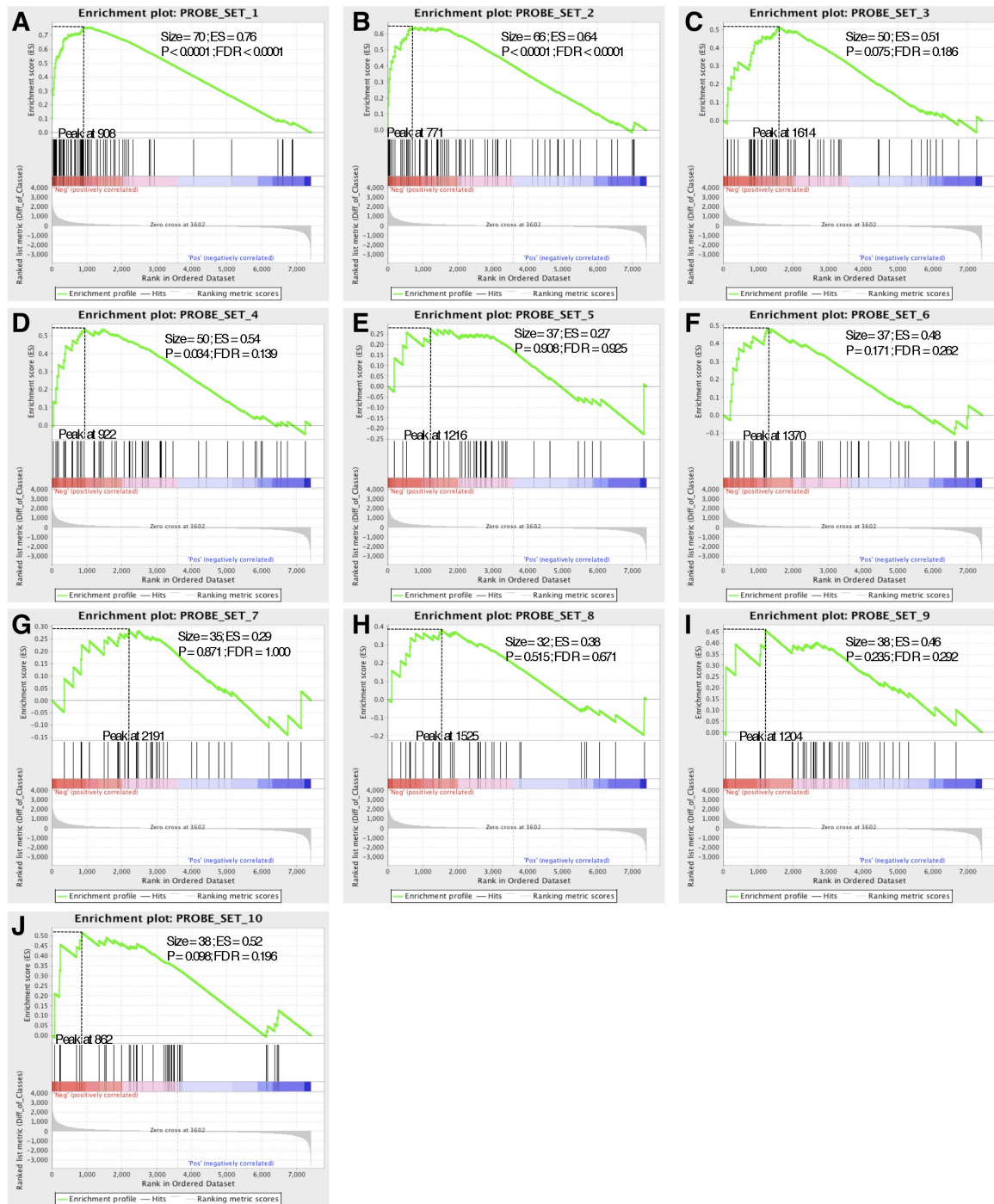


Figure S4. Enrichment analysis of the HOCTAR ranked list for miR-26b in the dataset of probes differentially expressed after miR-26b overexpression. Panels from A to J display the results obtained with ten bins (probe sets) in which the whole HOCTAR list was subdivided. Please note that only the probes ($n=7410$) showing significant expression variations ($FDR < 0.05$) in the microarray experiment are shown in these plots. See text for further details. Legend: Size= Number of probes displaying significant changes in their expression levels; ES = enrichment score; P = nominal P -value; FDR = False discovery Rate; Peak = the position in the ranked list at which the maximum enrichment score occurred.

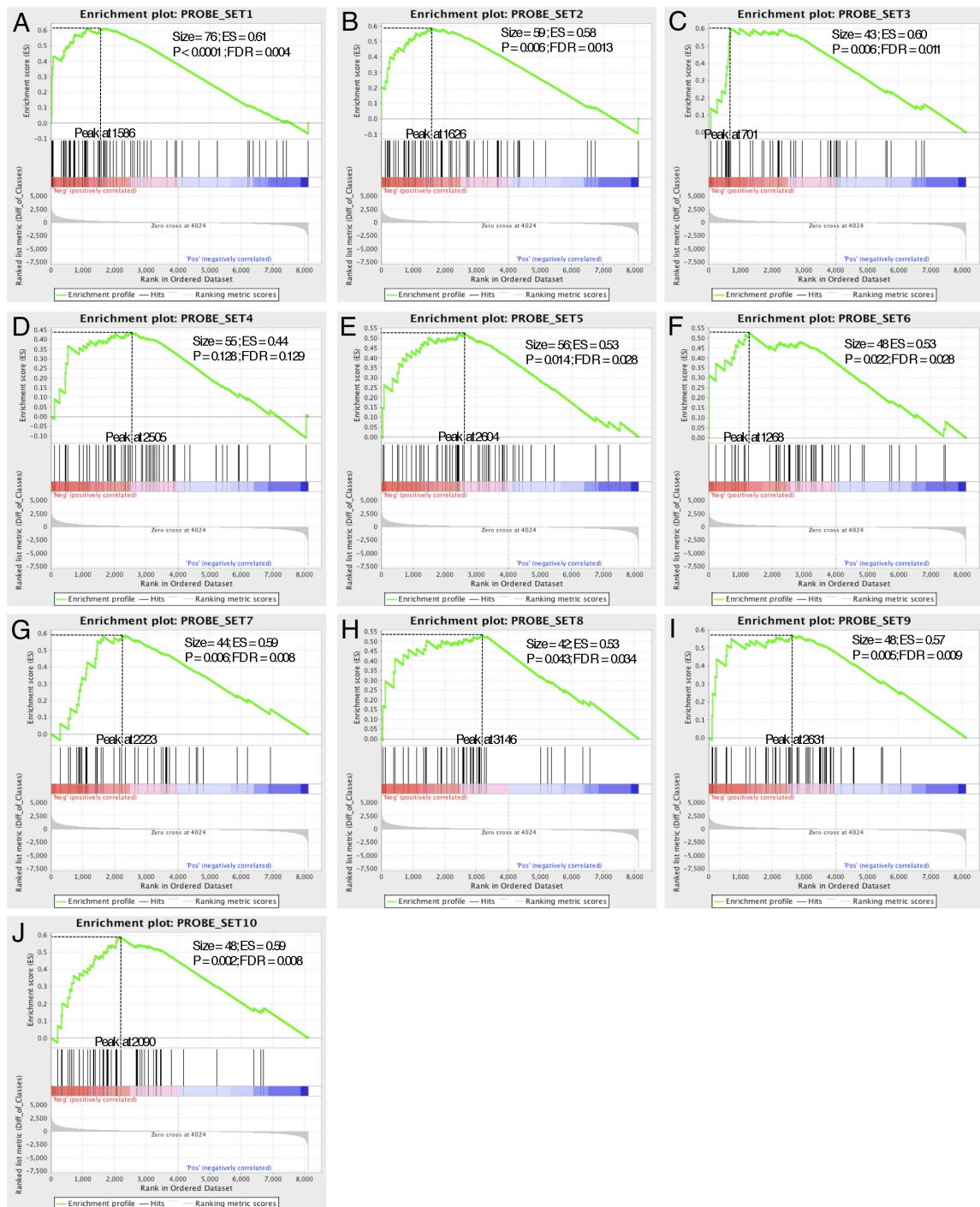


Figure S5. Enrichment analysis of the HOCTAR ranked list for miR-98 in the dataset of probes differentially expressed after miR-98 overexpression. Panels from A to J display the results obtained with ten bins (probe sets) in which the whole HOCTAR list was subdivided. Please note that only the probes ($n=8125$) showing significant expression variations ($FDR < 0.05$) in the microarray experiment are shown in these plots. See text for further details. Legend: Size= Number of probes displaying significant changes in their expression levels; ES = enrichment score; P = nominal P -value; in the gene set after filtering out those genes not in the expression dataset; FDR = False discovery Rate; Peak = the position in the ranked list at which the maximum enrichment score occurred.

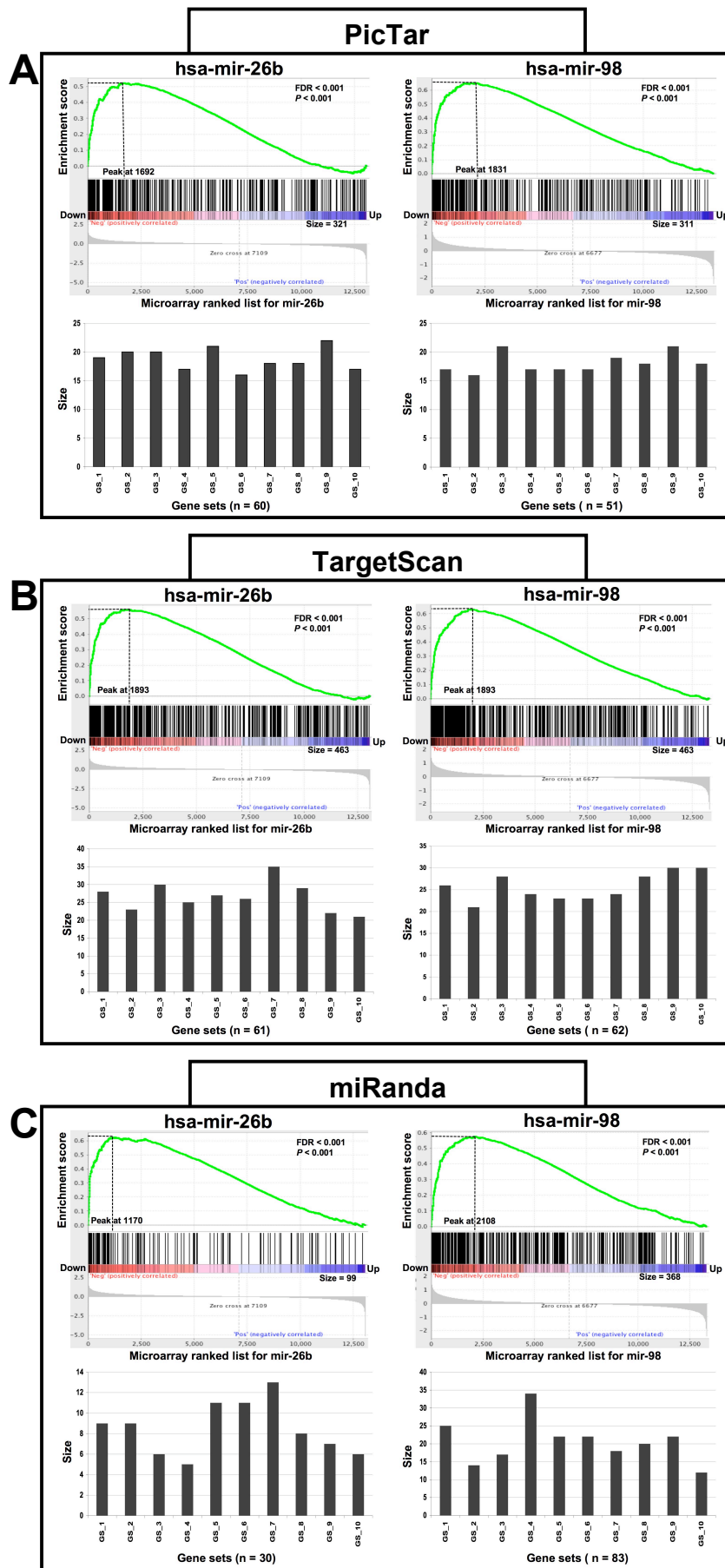


Figure S6. GSEA analysis on the ranked lists of prediction by PicTar, TargetScan and miRanda for both genes down-regulated after miR-26b and miR-98 overexpression. Enrichment plots and the gene size for each bin generated by GSEA analysis of the PicTar (panel A), TargetScan (panel B) and miRanda (panel C) predictions list for miR-26b and miR-98 are represented (see Fig. 4 for further details).

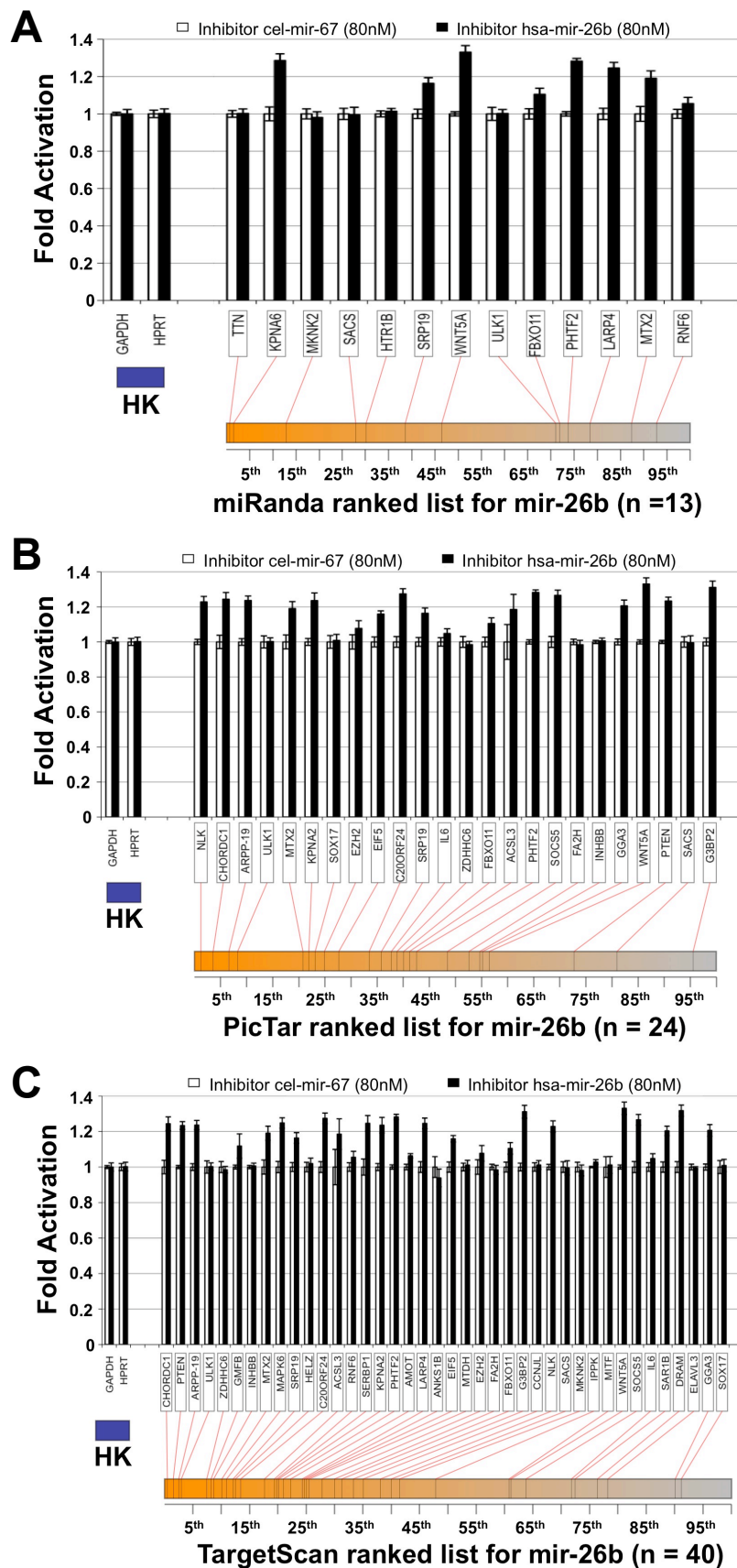


Figure S7. Distribution of the genes analyzed after downregulation of miR-26b in HeLa cells, as reported in Figure 5A, within the ranked lists of TargetScan, PicTar and miRanda for miR-26b. The histograms show the differences in the expression levels between HeLa cells transfected with a miRNA-inhibitor (black bars) and control (cel-miR-67 transfected) HeLa cells (white bars), of a subset of miRanda (panel A), PicTar (panel B) and TargetScan (panel C) predicted target genes for miR-26b. Y-axis: fold change activation (expressed as $2^{-\Delta\Delta C_t}$ values). X-axis: predicted target genes tested (their symbols are indicated in the boxes). The target genes tested were homogeneously distributed along the entire ranked lists pertaining to each of these prediction softwares and the red lines below the diagrams indicate the ranking of each target genes tested within miRanda (A), PicTar (B) and TargetScan (C) prediction lists for miR-26b. The HK indicate the house-keeping genes used to normalize the expression levels.

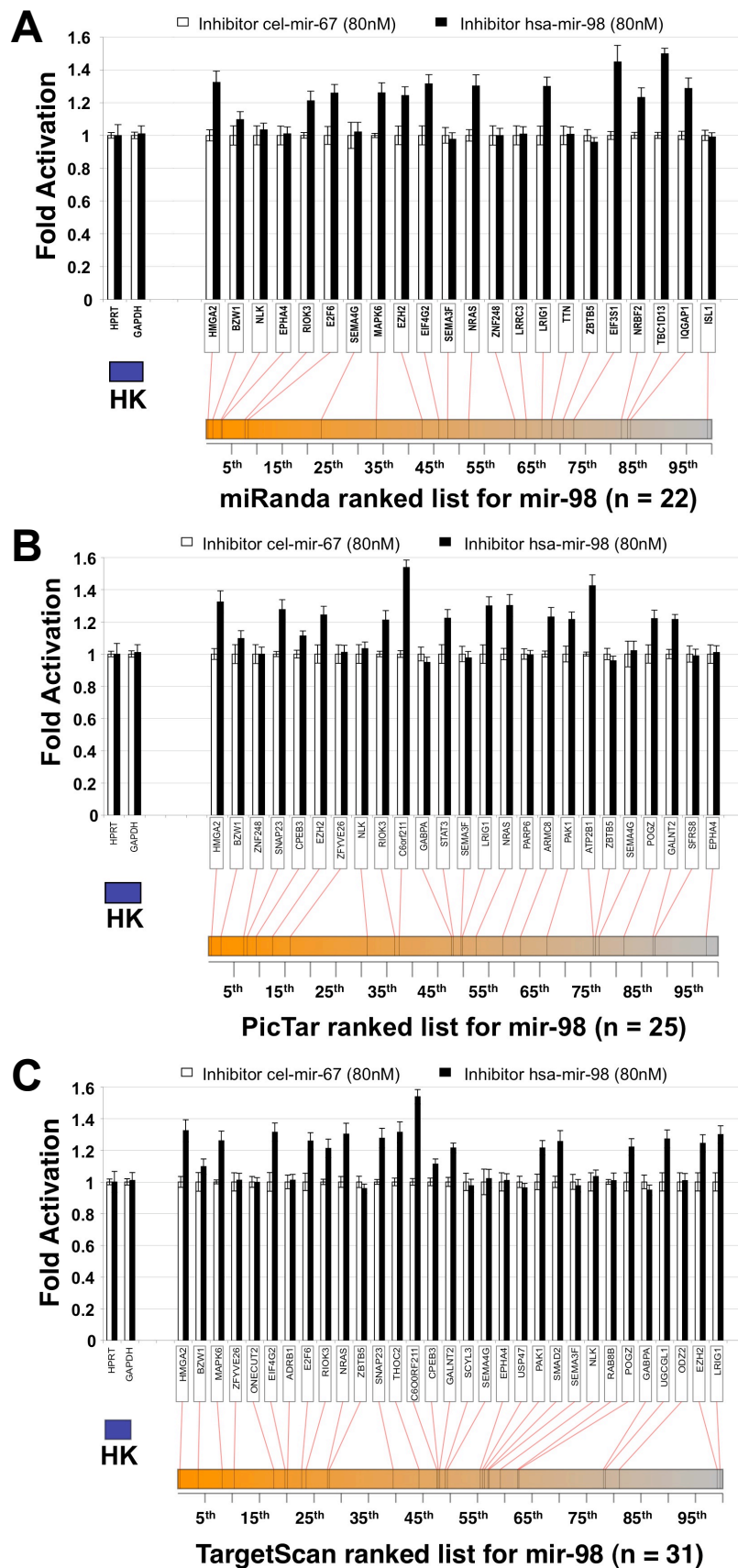


Figure S8. Distribution of the genes analyzed after downregulation of miR-98 in HeLa cells, as reported in Figure 5B, within the ranked lists of TargetScan, PicTar and miRanda for miR-98. The histograms show the differences in the expression levels between HeLa cells transfected with a miRNA-inhibitor (black bars) and control (cel-miR-67 transfected) HeLa cells (white bars), of a subset of miRanda (panel A), PicTar (panel B) and TargetScan (panel C) predicted target genes for miR-98. Y-axis: fold change activation (expressed as $2^{-\Delta\Delta C_t}$ values). X-axis: predicted target genes tested (their symbols are indicated in the boxes). The target genes tested were homogeneously distributed along the entire ranked lists pertaining to each of these prediction softwares and the red lines below the diagrams indicate the ranking of each target genes tested within miRanda (A), PicTar (B) and TargetScan (C) prediction lists for miR-98. The HK indicate the house-keeping genes used to normalize the expression levels.

Table S1. List of candidate miRNA-target pairs used for HOCTAR validation

miRNA	Host gene	Validated Target	Bibliographic Reference	Validation procedure
hsa-mir-101-2	<i>RCL1</i>	<i>MYCN</i>	(Lewis et al. 2003)	Translational
hsa-mir-106b	<i>MCM7</i>	<i>p21/CDKN1A</i>	(Ivanovska et al. 2008)	Translational Transcriptional
hsa-mir-128a	<i>R3HDM1</i>	<i>SNAP25</i>	(Eletto et al. 2008)	Translational
hsa-mir-140	<i>WWP2</i>	<i>PDGFRA</i>	(Clouthier 2008)	Translational
hsa-mir-15a	<i>DLEU2</i>	<i>CREBL2</i>	(Calin et al. 2008)	Translational Transcriptional
hsa-mir-15a	<i>DLEU2</i>	<i>PDCD4</i>	(Calin et al. 2008)	Translational Transcriptional
hsa-mir-15a	<i>DLEU2</i>	<i>RAD51C</i>	(Calin et al. 2008)	Translational Transcriptional
hsa-mir-15a	<i>DLEU2</i>	<i>WT1</i>	(Calin et al. 2008)	Translational Transcriptional
hsa-mir-15a	<i>DLEU2</i>	<i>BCL2</i>	(Cimmino et al. 2005)	Translational Transcriptional
hsa-mir-15a	<i>DLEU2</i>	<i>PDCD6IP</i>	(Calin et al. 2008)	Translational Transcriptional
hsa-mir-15a	<i>DLEU2</i>	<i>IGSF4</i>	(Calin et al. 2008)	Translational Transcriptional
hsa-mir-15b	<i>SMC4</i>	<i>CREBL2</i>	(Calin et al. 2008)	Translational Transcriptional
hsa-mir-15b	<i>SMC4</i>	<i>PDCD4</i>	(Calin et al. 2008)	Translational Transcriptional
hsa-mir-15b	<i>SMC4</i>	<i>BCL2</i>	(Cimmino et al. 2005)	Translational Transcriptional
hsa-mir-15b	<i>SMC4</i>	<i>IGSF4</i>	(Calin et al. 2008)	Translational Transcriptional
hsa-mir-15b	<i>SMC4</i>	<i>RAD51C</i>	(Calin et al. 2008)	Translational Transcriptional
hsa-mir-16-1	<i>DLEU2</i>	<i>CREBL2</i>	(Calin et al. 2008)	Translational Transcriptional
hsa-mir-16-1	<i>DLEU2</i>	<i>PDCD4</i>	(Calin et al. 2008)	Translational Transcriptional
hsa-mir-16-1	<i>DLEU2</i>	<i>RAD51C</i>	(Calin et al. 2008)	Translational Transcriptional
hsa-mir-16-1	<i>DLEU2</i>	<i>CGI-38</i>	(Kiriakidou et al. 2004)	Translational
hsa-mir-16-1	<i>DLEU2</i>	<i>WT1</i>	(Calin et al. 2008)	Translational Transcriptional
hsa-mir-16-1	<i>DLEU2</i>	<i>BCL2</i>	(Cimmino et al. 2005)	Translational Transcriptional
hsa-mir-16-1	<i>DLEU2</i>	<i>PDCD6IP</i>	(Calin et al. 2008)	Translational Transcriptional
hsa-mir-16-1	<i>DLEU2</i>	<i>IGSF4</i>	(Calin et al. 2008)	Translational Transcriptional
hsa-mir-16-2	<i>SMC4</i>	<i>CREBL2</i>	(Calin et al. 2008)	Translational Transcriptional
hsa-mir-16-2	<i>SMC4</i>	<i>PDCD6IP</i>	(Calin et al. 2008)	Translational Transcriptional
hsa-mir-16-2	<i>SMC4</i>	<i>CGI-38</i>	(Kiriakidou et al. 2004)	Translational
hsa-mir-16-2	<i>SMC4</i>	<i>PDCD4</i>	(Calin et al. 2008)	Translational Transcriptional

hsa-mir-16-2	<i>SMC4</i>	<i>BCL2</i>	(Cimmino et al. 2005)	Translational Transcriptional
hsa-mir-16-2	<i>SMC4</i>	<i>WT1</i>	(Calin et al. 2008)	Translational Transcriptional
hsa-mir-16-2	<i>SMC4</i>	<i>IGSF4</i>	(Calin et al. 2008)	Translational Transcriptional
hsa-mir-16-2	<i>SMC4</i>	<i>RAD51C</i>	(Calin et al. 2008)	Translational Transcriptional
hsa-mir-208a	<i>MYH6</i>	<i>THRAP1</i>	(van Rooij et al. 2007)	Translational Transcriptional
hsa-mir-208b	<i>MYH7</i>	<i>THRAP1</i>	(van Rooij et al. 2007)	Translational Transcriptional
hsa-mir-21	<i>TMEM49</i>	<i>PDCD4</i>	(Asangani et al. 2008)	Translational
hsa-mir-23b	<i>C9orf3</i>	<i>CXCL12</i>	(Lewis et al. 2003)	Translational
hsa-mir-23b	<i>C9orf3</i>	<i>POU4F2</i>	(Lewis et al. 2003)	Translational
hsa-mir-24-1	<i>C9orf3</i>	<i>MAPK14</i>	(Kiriakidou et al. 2004)	Translational
hsa-mir-24-1	<i>C9orf3</i>	<i>ACVR1B(ALK4)</i>	(Wang et al. 2008)	Translational
hsa-mir-24-1	<i>C9orf3</i>	<i>(CDKN2A)p16/INK4a</i>	(Lal et al. 2008)	Translational
hsa-mir-25	<i>MCM7</i>	<i>NFIB</i>	(Grimson et al. 2007)	Translational
hsa-mir-25	<i>MCM7</i>	<i>CDH10</i>	(Grimson et al. 2007)	Translational
hsa-mir-25	<i>MCM7</i>	<i>CCDC131(MGC23401)</i>	(Grimson et al., 2007)	Translational
hsa-mir-25	<i>MCM7</i>	<i>PHTF2</i>	(Grimson et al. 2007)	Translational
hsa-mir-25	<i>MCM7</i>	<i>DYRK2</i>	(Grimson et al. 2007)	Translational
hsa-mir-26a-1	<i>CTDSPL</i>	<i>EZH2</i>	(Wong and Tellam 2008)	Translational Transcriptional
hsa-mir-26a-1	<i>CTDSPL</i>	<i>SERBP1</i>	(Beitzinger et al. 2007)	Translational
hsa-mir-26a-2	<i>CTDSP2</i>	<i>SERBP1</i>	(Beitzinger et al. 2007)	Translational
hsa-mir-26a-2	<i>CTDSP2</i>	<i>EZH2</i>	(Wong and Tellam 2008)	Translational Transcriptional
hsa-mir-26b	<i>CTDSP1</i>	<i>SERBP1</i>	(Beitzinger et al. 2007)	Translational
hsa-mir-26b	<i>CTDSP1</i>	<i>EZH2</i>	(Wong and Tellam 2008)	Translational Transcriptional
hsa-mir-27b	<i>C9orf3</i>	<i>CYP1B1</i>	(Tsuchiya et al. 2006)	Translational
hsa-mir-33b	<i>SREBF1</i>	<i>FOXG1B</i>	(Bredenkamp et al. 2007)	Translational
hsa-mir-9-1	<i>C1orf61</i>	<i>FOXG1B</i>	(Bredenkamp et al. 2007)	Translational
hsa-mir-98	<i>HUWE1</i>	<i>HMGA2</i>	(Hebert et al. 2007)	Transcriptional
hsa-mir-98	<i>HUWE1</i>	<i>MYC</i>	(Sampson et al. 2007)	Transcriptional

REFERENCES

- Asangani, I.A., Rasheed, S.A., Nikolova, D.A., Leupold, J.H., Colburn, N.H., Post, S., and Allgayer, H. 2008. MicroRNA-21 (miR-21) post-transcriptionally downregulates tumor suppressor Pcd4 and stimulates invasion, intravasation and metastasis in colorectal cancer. *Oncogene* **27**(15): 2128-2136.
- Beitzinger, M., Peters, L., Zhu, J.Y., Kremmer, E., and Meister, G. 2007. Identification of human microRNA targets from isolated argonaute protein complexes. *RNA Biol* **4**(2): 76-84.
- Bredenkamp, N., Seoighe, C., and Illing, N. 2007. Comparative evolutionary analysis of the FoxG1 transcription factor from diverse vertebrates identifies conserved recognition sites for microRNA regulation. *Dev Genes Evol* **217**(3): 227-233.
- Calin, G.A., Cimmino, A., Fabbri, M., Ferracin, M., Wojcik, S.E., Shimizu, M., Taccioli, C., Zanesi, N., Garzon, R., Aqeilan, R.I. et al. 2008. MiR-15a and miR-16-1 cluster functions in human leukemia. *Proc Natl Acad Sci U S A* **105**(13): 5166-5171.
- Cimmino, A., Calin, G.A., Fabbri, M., Iorio, M.V., Ferracin, M., Shimizu, M., Wojcik, S.E., Aqeilan, R.I., Zupo, S., Dono, M. et al. 2005. miR-15 and miR-16 induce apoptosis by targeting BCL2. *Proc Natl Acad Sci U S A* **102**(39): 13944-13949.
- Clouthier, D.E. 2008. MicroRNAs in facial development. *Nat Genet* **40**(3): 268-269.
- Eletto, D., Russo, G., Passiatore, G., Del Valle, L., Giordano, A., Khalili, K., Gualco, E., and Peruzzi, F. 2008. Inhibition of SNAP25 expression by HIV-1 Tat involves the activity of mir-128a. *J Cell Physiol* **216**(3): 764-770.
- Grimson, A., Farh, K.K., Johnston, W.K., Garrett-Engele, P., Lim, L.P., and Bartel, D.P. 2007. MicroRNA targeting specificity in mammals: determinants beyond seed pairing. *Mol Cell* **27**(1): 91-105.
- Hebert, C., Norris, K., Scheper, M.A., Nikitakis, N., and Sauk, J.J. 2007. High mobility group A2 is a target for miRNA-98 in head and neck squamous cell carcinoma. *Mol Cancer* **6**: 5.
- Ivanovska, I., Ball, A.S., Diaz, R.L., Magnus, J.F., Kibukawa, M., Schelter, J.M., Kobayashi, S.V., Lim, L., Burchard, J., Jackson, A.L. et al. 2008. MicroRNAs in the miR-106b family regulate p21/CDKN1A and promote cell cycle progression. *Mol Cell Biol* **28**(7): 2167-2174.
- Kiriakidou, M., Nelson, P.T., Kouranov, A., Fitziev, P., Bouyioukos, C., Mourelatos, Z., and Hatzigeorgiou, A. 2004. A combined computational-experimental approach predicts human microRNA targets. *Genes Dev* **18**(10): 1165-1178.
- Lal, A., Kim, H.H., Abdelmohsen, K., Kuwano, Y., Pullmann, R., Jr., Srikantan, S., Subrahmanyam, R., Martindale, J.L., Yang, X., Ahmed, F. et al. 2008. p16(INK4a) translation suppressed by miR-24. *PLoS ONE* **3**(3): e1864.
- Lewis, B.P., Shih, I.H., Jones-Rhoades, M.W., Bartel, D.P., and Burge, C.B. 2003. Prediction of mammalian microRNA targets. *Cell* **115**(7): 787-798.
- Sampson, V.B., Rong, N.H., Han, J., Yang, Q., Aris, V., Soteropoulos, P., Petrelli, N.J., Dunn, S.P., and Krueger, L.J. 2007. MicroRNA let-7a down-regulates MYC and reverts MYC-induced growth in Burkitt lymphoma cells. *Cancer Res* **67**(20): 9762-9770.
- Tsuchiya, Y., Nakajima, M., Takagi, S., Taniya, T., and Yokoi, T. 2006. MicroRNA regulates the expression of human cytochrome P450 1B1. *Cancer Res* **66**(18): 9090-9098.
- van Rooij, E., Sutherland, L.B., Qi, X., Richardson, J.A., Hill, J., and Olson, E.N. 2007. Control of stress-dependent cardiac growth and gene expression by a microRNA. *Science (New York, NY)* **316**(5824): 575-579.

- Wang, Q., Huang, Z., Xue, H., Jin, C., Ju, X.L., Han, J.D., and Chen, Y.G. 2008. MicroRNA miR-24 inhibits erythropoiesis by targeting activin type I receptor ALK4. *Blood* **111**(2): 588-595.
- Wong, C.F. and Tellam, R.L. 2008. MicroRNA-26a targets the histone methyltransferase Enhancer of Zeste homolog 2 during myogenesis. *J Biol Chem* **283**(15): 9836-9843.

Table S2. Gene Ontology categories enriched in HOCTAR predictions

Host Gene	miRNA	Gene Ontology category	Fold Enrichment		
			100 th	50 th	30 th
RCL1	hsa-mir-101-2	regulation of gene expression, epigenetic	3.9	5.7	7.5
PANK3	hsa-mir-103-1	mesoderm formation	4.9	7.5	9.7
PANK3	hsa-mir-103-1	formation of primary germ layer	4.5	6.9	8.8
PANK3	hsa-mir-103-1	mesoderm morphogenesis	4.5	6.9	8.8
PANK2	hsa-mir-103-2	mesoderm formation	4.9	7.3	9.4
PANK2	hsa-mir-103-2	formation of primary germ layer	4.5	6.6	8.6
PANK2	hsa-mir-103-2	mesoderm morphogenesis	4.5	6.6	8.6
GABRA3	hsa-mir-105-1	mRNA metabolic process	2.4	2.9	4.4
GABRA3	hsa-mir-105-1	mRNA processing	2.4	2.8	4.3
GABRA3	hsa-mir-105-1	RNA splicing	2.4	2.9	4.5
GABRA3	hsa-mir-105-2	mRNA metabolic process	2.4	2.9	4.4
GABRA3	hsa-mir-105-2	mRNA processing	2.4	2.8	4.3
GABRA3	hsa-mir-105-2	RNA splicing	2.4	2.9	4.5
MCM7	hsa-mir-106b	negative regulation of cell growth	4	6	9.2
MCM7	hsa-mir-106b	negative regulation of progression through cell cycle	2.1	2.3	3.3
MCM7	hsa-mir-106b	interphase of mitotic cell cycle	3.3	4.3	4.7
R3HDM1	hsa-mir-128a	ossification	2.6	3.6	5.4
R3HDM1	hsa-mir-128a	biomineral formation	2.6	3.6	5.4
R3HDM1	hsa-mir-128a	bone remodeling	2.3	3.3	4.9
ARPP-21	hsa-mir-128b	mRNA catabolic process, nonsense-mediated decay	5.6	8.6	13.1
ARPP-21	hsa-mir-128b	mRNA catabolic process	4.8	7.4	11.2
PDE2A	hsa-mir-139	regulation of RNA metabolic process	10.9	16	24.5
PDE2A	hsa-mir-139	RNA splicing	3.4	4.9	7
PDE2A	hsa-mir-139	mRNA metabolic process	2.5	3.7	4.8
WWP2	hsa-mir-140	androgen receptor signaling pathway	15.5	18.9	30.7
WWP2	hsa-mir-140	steroid hormone receptor signaling pathway	10.5	12.9	20.9
WWP2	hsa-mir-140	regulation of gene expression, epigenetic	8.3	12.6	20.4
WWP2	hsa-mir-140	intracellular receptor-mediated signaling pathway	9.9	12.1	19.6
COPZ1	hsa-mir-148b	positive regulation of cellular metabolic process	2.7	2.6	3.3
PTPRN	hsa-mir-153-1	N-terminal protein amino acid modification	9.8	15.3	26.2
DLEU2	hsa-mir-15a	negative regulation of protein amino acid phosphorylation	7.5	11.6	17.3
DLEU2	hsa-mir-15a	negative regulation of tyrosine phosphorylation of Stat3 protein	9.1	14	20.7
DLEU2	hsa-mir-15a	negative regulation of JAK-STAT cascade	7.8	12	17.8
SMC4	hsa-mir-15b	positive regulation of epithelial cell proliferation	5.5	8.5	12.8
SMC4	hsa-mir-16-2	regulation of cellular component organization and biogenesis	2.6	3.3	3.9
SMC4	hsa-mir-16-2	Wnt receptor signaling pathway	2.4	3	3.4
FSTL1	hsa-mir-198	chromatin-mediated maintenance of transcription	23.9	36.3	55.1
FSTL1	hsa-mir-198	positive regulation of gene expression, epigenetic	15.9	24.2	36.7
TRPM3	hsa-mir-204	small GTPase mediated signal transduction	1.9	2.6	3.5
MYH6	hsa-mir-208a	regulation of translational initiation	8.5	13.4	19.6
MYH6	hsa-mir-208a	protein-RNA complex assembly	4.4	6.8	10.1
MYH6	hsa-mir-208b	RNA splicing	4	5.7	7.2
MYH6	hsa-mir-208b	mRNA processing	3.8	5.5	7.1
MYH6	hsa-mir-208b	mRNA metabolic process	3.3	4.7	6.1
TMEM49	hsa-mir-21	positive regulation of gene expression, epigenetic	36.8	54.2	83.1
TRPM1	hsa-mir-211	MAPKKK cascade	2.2	2.7	3.6
SLIT2	hsa-mir-218-1	dephosphorylation	3.2	4.7	5.4
C17orf91	hsa-mir-22	positive regulation of nucleobase, nucleoside, nucleotide and nucleic acid metabolic process	2	2.1	2.4
GABRE	hsa-mir-224	mRNA metabolic process	2.2	3	4.5
GABRE	hsa-mir-224	mRNA processing	2.4	3.2	4.8
GABRE	hsa-mir-224	RNA splicing	2.3	3.1	4.2
C9orf3	hsa-mir-23b	chromatin modification	2.4	2.9	3.4
MCM7	hsa-mir-25	regulation of cell-matrix adhesion	8.2	12.3	18.3
CTDSPL	hsa-mir-26a-1	striated muscle development	3.6	4	5.5
CTDSPL	hsa-mir-26a-1	lymphocyte differentiation	3	4.4	6
CTDSP2	hsa-mir-26a-2	cell division	1.8	2.5	3.6
CTDSP1	hsa-mir-26b	microtubule depolymerization	9.6	14.3	23.6
CTDSP1	hsa-mir-26b	negative regulation of microtubule depolymerization	8.3	12.4	20.4
CTDSP1	hsa-mir-26b	microtubule polymerization or depolymerization	6.2	9.3	15.3
CTDSP1	hsa-mir-26b	negative regulation of cellular component organization and biogenesis	3.6	5.3	8.8
CTDSP1	hsa-mir-26b	microtubule cytoskeleton organization and biogenesis	3	4.5	7.4

C9orf3	hsa-mir-27b	positive regulation of cell differentiation	4	5.5	7.3
C9orf3	hsa-mir-27b	positive regulation of development process	3.7	4.6	5.6
NFYC	hsa-mir-30e	pattern specification process	2.6	2.6	3.9
C9orf5	hsa-mir-32	small GTPase mediated signal transduction	1.5	2	2.7
EML2	hsa-mir-330	mRNA splice site selection	11.1	16.4	20
EML2	hsa-mir-330	actin filament polymerization	5.5	8.2	12.5
EML2	hsa-mir-330	actin polymerization and/or depolymerization	3.6	5.3	8.1
SREBF2	hsa-mir-33a	cell growth	2.3	3.5	5.1
PPARGC1B	hsa-mir-378	regulation of Ras protein signal transduction	2.2	3	3.8
PPARGC1B	hsa-mir-378	regulation of small GTPase mediated signal transduction	2.1	2.6	3.4
HTR2C	hsa-mir-448	small GTPase mediated signal transduction	1.8	2.6	3.4
IGF2	hsa-mir-483	nuclear mRNA splicing, via spliceosome	9.5	14.5	20.4
IGF2	hsa-mir-483	RNA splicing, via transesterification reactions with bulged adenosine as nucleophile	9.5	14.5	20.4
ANK1	hsa-mir-486	enzyme linked receptor protein signaling pathway	3.6	5.2	7.5
CALCR	hsa-mir-489	protein import into nucleus	6.4	10.7	12.6
CALCR	hsa-mir-489	protein targeting	3.6	6.1	7.5
CHRM2	hsa-mir-490	mRNA metabolic process	3.6	5.3	7.5
MYH7B	hsa-mir-499	mRNA processing	3.9	5	6.3
MYH7B	hsa-mir-499	RNA splicing	4.1	5.1	6.3
MYH7B	hsa-mir-499	mRNA metabolic process	3.3	4.3	5.4
CLCN5	hsa-mir-532	mRNA metabolic process	3.6	5.2	7.5
FLJ20837	hsa-mir-548c	nuclear mRNA splicing, via spliceosome	2.3	3.4	4.8
FLJ20837	hsa-mir-548c	RNA splicing, via transesterification reactions with bulged adenosine as nucleophile	2.3	3.4	4.8
NOS1AP	hsa-mir-556	ubiquitin cycle	3.6	5	7.2
GULP1	hsa-mir-561	regulation of mRNA stability	11.6	17.8	26
GULP1	hsa-mir-561	mRNA stabilization	23.8	35.9	56
TNIK	hsa-mir-569	cell cycle	1.7	2.2	3.1
TNIK	hsa-mir-569	mRNA processing	2.9	3.7	5.1
SEC24B	hsa-mir-576	odontogenesis of dentine-containing teeth	7.8	11.6	16.3
SEC24B	hsa-mir-576	odontogenesis	6.6	9.8	13.8
CPE	hsa-mir-578	protein kinase cascade	2.1	2.9	4.4
CPE	hsa-mir-578	protein amino acid phosphorylation	2.8	3.3	3.5
ZFR	hsa-mir-579	transmembrane protein tyrosine kinase signaling pathway	2.4	2.9	3.8
ZFR	hsa-mir-579	mRNA metabolic process	2.2	2.6	3.5
ZFR	hsa-mir-579	mRNA processing	2.2	2.5	3.3
FBXL18	hsa-mir-589	histone modification	7.5	9.2	15.9
FBXL18	hsa-mir-589	RNA transport	5	7.4	11
FBXL18	hsa-mir-589	RNA splicing	3	4.4	7.6
SLC25A13	hsa-mir-591	negative regulation of transcription	6.6	8.1	8.9
SLC25A13	hsa-mir-591	negative regulation of nucleobase, nucleoside and nucleic metabolic process	6	7.4	8.1
SND1	hsa-mir-593	regulation of the force of heart contraction	24.4	40.7	65.5
C9orf45	hsa-mir-600	negative regulation of transcription from RNA polymerase II promoter	5.5	8.2	9.3
C10orf79	hsa-mir-609	regulation of transcription, DNA-dependent	2.6	2.8	3.2
APOLD1	hsa-mir-613	mRNA metabolic process	2.6	3.3	4.1
DDIT3	hsa-mir-616	protein complex assembly	2.5	3	4.2
PRKCA	hsa-mir-634	mRNA metabolic process	3.4	4	5.9
SFRS2	hsa-mir-636	neuron development	2.8	3.7	5.1
SFRS2	hsa-mir-636	neuron differentiation	2.4	2.9	4
DAPK3	hsa-mir-637	mRNA metabolic process	2.6	4.3	5.8
GATAD2A	hsa-mir-640	mRNA splice site selection	36.3	53.7	75.7
GATAD2A	hsa-mir-640	nuclear mRNA splicing, via spliceosome	13.8	20.4	28.9
GATAD2A	hsa-mir-640	RNA splicing, via transesterification reactions with bulged adenosine as nucleophile	13.8	20.4	28.9
AKT2	hsa-mir-641	mRNA metabolic process	1.7	2.7	4
CALCR	hsa-mir-653	ubiquitin cycle	2.3	3.4	3.8
CALCR	hsa-mir-653	negative regulation of transcription	2.5	3.2	4.3
CSG1cA-T	hsa-mir-671	regulation of cellular component organization and biogenesis	4.9	7.5	12.2
AP1G1	hsa-mir-768-3p	regulation of glial cell differentiation	71	96.6	140.5
CA12	hsa-mir-768-5p	positive regulation of cell differentiation	14.1	17.2	26.5
CA12	hsa-mir-768-5p	regulation of cell differentiation	6.9	9.2	12.2
CA12	hsa-mir-768-5p	regulation of developmental process	4.4	5.8	7.7
C1orf61	hsa-mir-9-1	regulation of Ras protein signal transduction	2.2	2.6	3.6
C1orf61	hsa-mir-9-1	mRNA splice site selection	6.5	10.2	15.7
MCM7	hsa-mir-93	interphase of mitotic cell cycle	3.3	4.5	5.1
MCM7	hsa-mir-93	blood vessel morphogenesis	2.4	3.4	3.9

MCM7	hsa-mir-93	angiogenesis	2.4	3.3	3.6
HUWE1	hsa-mir-98	fat cell differentiation	6.5	8	12
HUWE1	hsa-mir-98	steroid hormone receptor signaling pathway	3.1	4.7	6.1
HUWE1	hsa-mir-98	phosphate transport	3.9	4.8	5.9
HUWE1	hsa-let-7f-2	fat cell differentiation	6.4	8	11.8
HUWE1	hsa-let-7f-2	steroid hormone receptor signaling pathway	3.1	4.6	6
HUWE1	hsa-let-7f-2	phosphate transport	3.2	4.4	5.8

Table S3. Description list for all 160 different experiments in HG-U133A (GPL96) platform.

GEO	Dataset	Title
GDS1036.soft	GDS1036 - GPL96	Microglial cell response to interferon-gamma: time course
GDS1041.soft	GDS1041 - GPL96	CREB, CREMalpha, CREMtau2alpha, ATF2, and ATF2-small overexpression effect on myometrial cells
GDS1050.soft	GDS1050 - GPL96	Valproic acid effect on theca cells (HG-U133A)
GDS1062.soft	GDS1062 - GPL96	Squamous cell carcinoma of the oral cavity with lymph node metastasis
GDS1063.soft	GDS1063 - GPL96	Primary effusion lymphomas and associated viral infections
GDS1064.soft	GDS1064 - GPL96	Acute myeloid leukemia subclasses
GDS1065.soft	GDS1065 - GPL96	Mitochondrial encephalomyopathies associated with mitochondrial DNA mutations
GDS1067.soft	GDS1067 - GPL96	Plasma cell dyscrasias
GDS1069.soft	GDS1069 - GPL96	Homeobox gene HOXA5 induction: time course
GDS1096.soft	GDS1096 - GPL96	Normal tissues of various types
GDS1204.soft	GDS1204 - GPL96	Lung cancer cell line response to motexafin gadolinium: time course
GDS1209.soft	GDS1209 - GPL96	Sarcoma and hypoxia
GDS1215.soft	GDS1215 - GPL96	Acute myeloblastic leukemia cells response to all trans retinoic acid and valproic acid
GDS1220.soft	GDS1220 - GPL96	Malignant pleural mesothelioma
GDS1230.soft	GDS1230 - GPL96	Hematopoietic stem cell and progenitor cell comparison (HG-U133A)
GDS1250.soft	GDS1250 - GPL96	Atypical ductal hyperplasia and breast cancer
GDS1253.soft	GDS1253 - GPL96	Pituitary adenoma subtypes
GDS1257.soft	GDS1257 - GPL96	Sickle cell plasma effect on pulmonary artery endothelial cells (HG-U133A)
GDS1259.soft	GDS1259 - GPL96	Dermatomyositis
GDS1282.soft	GDS1282 - GPL96	Clear cell sarcoma of the kidney
GDS1284.soft	GDS1284 - GPL96	Multiple myeloma molecular classification
GDS1286.soft	GDS1286 - GPL96	Esophageal cell response to low pH: time course
GDS1287.soft	GDS1287 - GPL96	Bone mineral density and circulating monocytes
GDS1288.soft	GDS1288 - GPL96	Mesenchymal precursor cells derived from embryonic stem cells
GDS1295.soft	GDS1295 - GPL96	Lethal congenital contracture syndrome
GDS1304.soft	GDS1304 - GPL96	Cigarette smoking effect on small airway epithelium
GDS1312.soft	GDS1312 - GPL96	Squamous lung cancer
GDS1313.soft	GDS1313 - GPL96	GFAP-negative lamina cribrosa cell response to TGF-beta1
GDS1314.soft	GDS1314 - GPL96	Malignant melanoma cell lines
GDS1317.soft	GDS1317 - GPL96	Umbilical vein endothelial cell response to shear stress and intraluminal pressure
GDS1321.soft	GDS1321 - GPL96	Barrett's metaplasia progression to adenocarcinoma
GDS1324.soft	GDS1324 - GPL96	T-cell acute lymphoblastic leukemia with CALM-AF10 fusion
GDS1325.soft	GDS1325 - GPL96	Telomerase reverse transcriptase overexpression effect on CD4+ lymphocytes
GDS1326.soft	GDS1326 - GPL96	Breast cancer cells reexpressing estrogen receptor alpha response to 17beta-estradiol
GDS1327.soft	GDS1327 - GPL96	Lens epithelial and lens cortical fiber cell comparison
GDS1329.soft	GDS1329 - GPL96	Molecular apocrine breast tumors
GDS1331.soft	GDS1331 - GPL96	Huntington's disease: peripheral blood expression profile (HG-U133A)
GDS1333.soft	GDS1333 - GPL96	Duchenne Muscular Dystrophy response to oxandrolone (HG-U133A)
GDS1340.soft	GDS1340 - GPL96	Exercise effect on aged muscle
GDS1353.soft	GDS1353 - GPL96	Glucocorticoid effect on lens epithelial cells: time course
GDS1355.soft	GDS1355 - GPL96	Pancreatic ductal carcinoma (HG-U133A)
GDS1362.soft	GDS1362 - GPL96	Ischemic and nonischemic cardiomyopathy comparison
GDS1373.soft	GDS1373 - GPL96	Peroxisome proliferator-activated receptor subtype activation effect on liver cell
GDS1375.soft	GDS1375 - GPL96	Cutaneous malignant melanoma
GDS1376.soft	GDS1376 - GPL96	Essential thrombocythemia
GDS1380.soft	GDS1380 - GPL96	Glioblastoma pseudopalisading cells
GDS1384.soft	GDS1384 - GPL96	c-Myb and its oncogenic variant v-Myb
GDS1386.soft	GDS1386 - GPL96	Colorectal carcinoma subtype with microsatellite instability (HG-U133A)
GDS1390.soft	GDS1390 - GPL96	Prostate cancer progression after androgen ablation
GDS1392.soft	GDS1392 - GPL96	Myelodysplastic syndrome
GDS1397.soft	GDS1397 - GPL96	T cells infected with an HIV-based vector
GDS1401.soft	GDS1401 - GPL96	CD34+ hematopoietic cells expanded in artificial matrix of fibrillar collagen I
GDS1405.soft	GDS1405 - GPL96	Pulmonary type II cell differentiation

GDS1414.soft	GDS1414 - GPL96	Candoxin effect on glial cells: time course
GDS1423.soft	GDS1423 - GPL96	Lunasin effect on prostate epithelial cells
GDS1426.soft	GDS1426 - GPL96	Transcription factor HNF4alpha role in renal cell carcinoma
GDS1428.soft	GDS1428 - GPL96	Neutrophil response to Anaplasma phagocytophilum infection: time course
GDS1438.soft	GDS1438 - GPL96	Kidneys removed by laparoscopic donor nephrectomy
GDS1447.soft	GDS1447 - GPL96	Bronchial epithelial cell response to vanadium and zinc
GDS1453.soft	GDS1453 - GPL96	Camptothecin effect on renal epithelial cell line and HIV transduction
GDS1461.soft	GDS1461 - GPL96	Retinoic acid effect on conjunctival epithelial cells: time course
GDS1476.soft	GDS1476 - GPL96	Uterine fibroids with fumarate hydratase mutations
GDS1477.soft	GDS1477 - GPL96	Transcription factor FoxM1 inactivation effect on breast cancer cell
GDS1478.soft	GDS1478 - GPL96	Intestinal epithelial cell response to probiotic Escherichia coli strain Nissle 1917
GDS1479.soft	GDS1479 - GPL96	Carcinoma in situ lesions of the urinary bladder
GDS1480.soft	GDS1480 - GPL96	Obesity: preadipocyte expression profile (HG-U133A)
GDS1499.soft	GDS1499 - GPL96	Hepatocyte nuclear factor 1beta mutant overexpression effect on embryonic kidney cells
GDS1503.soft	GDS1503 - GPL96	Hutchinson-Gilford progeria syndrome: fibroblast (HG-U133A)
GDS1505.soft	GDS1505 - GPL96	Cultured skin substitute
GDS1542.soft	GDS1542 - GPL96	Tumor necrosis factor effect on macrovascular umbilical vein endothelial cells
GDS1543.soft	GDS1543 - GPL96	Tumor necrosis factor effect on microvascular endothelial cells
GDS1548.soft	GDS1548 - GPL96	Neuroblastoma cell lines
GDS1549.soft	GDS1549 - GPL96	Estrogen effect on estrogen receptor alpha positive breast cancer cell lines
GDS1556.soft	GDS1556 - GPL96	Atrial and ventricular myocardium comparison (HG-U133A)
GDS1558.soft	GDS1558 - GPL96	Permanent atrial fibrillation (HG-U133A)
GDS1615.soft	GDS1615 - GPL96	Ulcerative colitis and Crohn's disease comparison: peripheral blood mononuclear cells
GDS1618.soft	GDS1618 - GPL96	Lymph node and tonsil comparison
GDS1630.soft	GDS1630 - GPL96	Immortalized endothelial cell line response to atorvastatin
GDS1637.soft	GDS1637 - GPL96	Oncogene-induced senescence in vitro model
GDS1663.soft	GDS1663 - GPL96	Expression data from different research centers
GDS1664.soft	GDS1664 - GPL96	Parathyroid hormone-related protein knockdown effect on breast cancer cells
GDS1684.soft	GDS1684 - GPL96	Cardiac allograft rejection: time course
GDS1688.soft	GDS1688 - GPL96	Various lung cancer cell lines
GDS1713.soft	GDS1713 - GPL96	Ewing family tumor and neuroblastoma comparison
GDS1736.soft	GDS1736 - GPL96	Arachidonic acid effect on prostate cancer cells
GDS1746.soft	GDS1746 - GPL96	Primary epithelial cell cultures from prostate tumors
GDS1750.soft	GDS1750 - GPL96	Mantle cell lymphoma cell lines (HG-U133A)
GDS1758.soft	GDS1758 - GPL96	Pterygium
GDS1775.soft	GDS1775 - GPL96	Major leukocyte types
GDS1780.soft	GDS1780 - GPL96	Colorectal cancer progression: polysomal mRNA profiles
GDS1783.soft	GDS1783 - GPL96	Vascular smooth muscle response to voltage-dependent and store-operated calcium channel activation
GDS1791.soft	GDS1791 - GPL96	Wilms' tumor
GDS1806.soft	GDS1806 - GPL96	Modeled microgravity effect on activated T lymphocytes
GDS1841.soft	GDS1841 - GPL96	Chronic endoplasmic reticulum stress imposed by misfolded surfactant protein C (HG-U133A)
GDS1942.soft	GDS1942 - GPL96	Transgenic KrÄ¼ppel-like factor 4 induction: time course
GDS1965.soft	GDS1965 - GPL96	Melanocyte to melanoma transformation
GDS1971.soft	GDS1971 - GPL96	Uncomplicated and complicated malaria: whole blood
GDS1975.soft	GDS1975 - GPL96	Gliomas of grades III and IV (HG-U133A)
GDS1979.soft	GDS1979 - GPL96	Amyloid precursor protein intracellular domain effect on neural cells
GDS2039.soft	GDS2039 - GPL96	Endothelial cell morphogenesis (HG-U133A)
GDS2055.soft	GDS2055 - GPL96	Skeletal muscle types (HG-U133A)
GDS2057.soft	GDS2057 - GPL96	Androgen receptor modulator effect: time course (HG-U133A)
GDS2113.soft	GDS2113 - GPL96	Pheochromocytomas of various genetic origins
GDS2175.soft	GDS2175 - GPL96	Cockayne syndrome group B protein-null fibroblast rescue (HG-U133A)
GDS2190.soft	GDS2190 - GPL96	Bipolar disorder: dorsolateral prefrontal cortex
GDS2191.soft	GDS2191 - GPL96	Bipolar disorder: orbitofrontal cortex
GDS2367.soft	GDS2367 - GPL96	Tamoxifen effect on breast cancer cell line expressing estrogen receptor alpha and beta
GDS266.soft	GDS266 - GPL96	Asthma and atopy (HG-U133A)

GDS268.soft	GDS268 - GPL96	Obesity and fatty acid oxidation
GDS287.soft	GDS287 - GPL96	Muscle function and aging - male (HG-U133A)
GDS289.soft	GDS289 - GPL96	Chronic obstructive pulmonary disease
GDS395.soft	GDS395 - GPL96	Biomaterial engineering
GDS420.soft	GDS420 - GPL96	Severe combined immunodeficiency (HG-U133A)
GDS462.soft	GDS462 - GPL96	Heart failure and left ventricular assist device support
GDS472.soft	GDS472 - GPL96	Muscle function and aging - female (HG-U133A)
GDS484.soft	GDS484 - GPL96	Uterine fibroid and normal myometrial tissue
GDS493.soft	GDS493 - GPL96	Cystic fibrosis pathology and 4-phenylbutyrate (HG-U133A)
GDS505.soft	GDS505 - GPL96	Renal clear cell carcinoma (HG-U133A)
GDS513.soft	GDS513 - GPL96	Familial combined hyperlipidemia and USF1 haplotype
GDS525.soft	GDS525 - GPL96	Extraocular and limb muscle comparison
GDS534.soft	GDS534 - GPL96	Smoking-induced changes in airway transcriptome
GDS536.soft	GDS536 - GPL96	Androgen receptor antagonist to agonist conversion
GDS552.soft	GDS552 - GPL96	Essential thrombocythemia megakaryocytes
GDS558.soft	GDS558 - GPL96	Myocardial remodeling in response to LVAD
GDS559.soft	GDS559 - GPL96	Inflammatory bowel disease (HG-U133A)
GDS561.soft	GDS561 - GPL96	Osteopontin overexpression
GDS562.soft	GDS562 - GPL96	Bone cell tissue culture on amino acid conjugated surfaces
GDS564.soft	GDS564 - GPL96	Sex specific transcription in hypothalamus
GDS596.soft	GDS596 - GPL96	Large-scale analysis of the human transcriptome (HG-U133A)
GDS649.soft	GDS649 - GPL96	Inflammatory response of interleukin-1-stimulated endothelial cells
GDS686.soft	GDS686 - GPL96	Store-operated calcium entry in HEK-293 cells
GDS690.soft	GDS690 - GPL96	Intestinal epithelial cell immune response
GDS715.soft	GDS715 - GPL96	Acute myeloid leukemia cell differentiation induced by various drugs
GDS731.soft	GDS731 - GPL96	Leukotriene LTD4 effect on macrophage and endothelial cells
GDS737.soft	GDS737 - GPL96	Lung tissue from smokers with severe emphysema
GDS738.soft	GDS738 - GPL96	Intervertebral disc cells and osmotic loading
GDS748.soft	GDS748 - GPL96	Beta-catenin S37A mutant effect on gene expression
GDS749.soft	GDS749 - GPL96	Sarcopenia expression profiling
GDS756.soft	GDS756 - GPL96	Colon cancer progression
GDS760.soft	GDS760 - GPL96	T-cell acute lymphoblastic leukemia and T-cell lymphoblastic lymphoma comparison
GDS761.soft	GDS761 - GPL96	Essential thrombocythemia expression profiling
GDS785.soft	GDS785 - GPL96	CD4+ T cell differentiation (HG-133A)
GDS810.soft	GDS810 - GPL96	Alzheimer's disease at various stages of severity
GDS820.soft	GDS820 - GPL96	Breast cancer cell expression profiles (HG-U133A)
GDS826.soft	GDS826 - GPL96	Erythroid differentiation of erythroleukemia cell line induced by hemin: time course
GDS834.soft	GDS834 - GPL96	Sindbis virus-induced cell death
GDS855.soft	GDS855 - GPL96	Transforming growth factor beta effect on CD34+ hematopoietic stem cells
GDS858.soft	GDS858 - GPL96	Mucoid and motile Pseudomonas aeruginosa infected lung epithelial cell comparison
GDS860.soft	GDS860 - GPL96	Endothelin-1 effect on fibroblasts
GDS885.soft	GDS885 - GPL96	Tumor cell response to topoisomerase poison camptothecin
GDS901.soft	GDS901 - GPL96	Estrogen receptor alpha L540Q mutation effect on gene induction by estradiol: time course
GDS906.soft	GDS906 - GPL96	Bladder smooth muscle cell response to mechanical stretch
GDS914.soft	GDS914 - GPL96	Metabolic syndrome response to exercise intervention (HG-U133A)
GDS916.soft	GDS916 - GPL96	Ewing family tumor histogenetic origin
GDS917.soft	GDS917 - GPL96	Whole blood RNA isolation and leukocyte RNA purification: comparison of methods
GDS940.soft	GDS940 - GPL96	Kaposi sarcoma-associated herpesvirus infection of primary human dermal endothelial cells
GDS946.soft	GDS946 - GPL96	Familial combined hyperlipidemia
GDS962.soft	GDS962 - GPL96	Peripheral blood mononuclear cells and the effect of exercise
GDS987.soft	GDS987 - GPL96	Kidney transplant response to calcineurin inhibitor-free immunosuppression using sirolimus
GDS992.soft	GDS992 - GPL96	Endoplasmic reticulum membrane-associated genes in breast cancer cell line MCF-7

Table S4. List of primer used to validate HOCTAR ranked list hsa-mir-26b

Genes	Forward	Reverse
<i>HPRT1</i>	TGGACAGGACTGAACGTCTTGC	TTATAGCCCCCCTTGAGCACA
<i>GAPDH</i>	ACTTCAACAGCGACACCCACT	GCCAAATTCGTTGTCATACCAG
<i>ARPP-19</i>	AGGAAACGGTTGCAGAAAGG	GTCTTGCGGAGTGGGAATGT
<i>KPNA2</i>	TCCAAGCTACTCAAGCTGCCAG	CCAGCCCGGATTATGTTGTCT
<i>RNF6</i>	TCTTTTAGGCACCCCTGGAGA	GCTAGTTGTTCTTGACGCCAT
<i>GMFB</i>	GGTGGTACTGGATGAGGAGCTT	GAATCGAGGTTGTCGTTCAGG
<i>MTX2</i>	TGCTGTTGACTGCAGAGCTGT	CCTAGCATGAGTGATCTCCCCT
<i>MTDH</i>	CCTCTAAAACCCGTCCAAAACA	TCGGTAGAAGTAGCAGGTGGAA
<i>G3BP2</i>	CAAACCTTTGTTCTGGCTCCT	AGTTCAGGCTCAGAATCACCA
<i>EIF5</i>	CGTCTGATTGCCAAGGTTGAG	TGCAACGTCAACCATGTTGAC
<i>SERBP1</i>	TCAAAGAGTGAAGAGGCTCATGC	GGTCTCCAAAATTGATCTCCAGC
<i>RCN2</i>	TTGATCCCCAAGAGCTGTTACC	CAATTAGATGAAGCGCCTCCTC
<i>CHORDC1</i>	ATGGCCTTGCTGTGCTACAAC	GACCAACCCTTTAATGCATCGT
<i>SAR1B</i>	CCAACATTACATCCCCTTCCG	TGAACATGTCCACCCAGATCAA
<i>LARP4</i>	GCTCTACAGGAACCCCGAAAGT	CGTAGTGGCTGCACAAGAAGT
<i>MAPK6</i>	GACATGACTGAGCCACACAAA	CTTCTGCTGTTAACCGATCCA
<i>C20orf24</i>	CTGGTTCCGACAGATCATTGC	CCTGCATTGATCAGGCAGAAT
<i>SRP19</i>	GGCGAATCCCCATAAGTAAGG	TGGACATCACGATTCCATTCTC
<i>PHTF2</i>	CATTACCCTAATGAGGACGCCC	GCCTTGCACTCTCAGAATCCTG
<i>SOCS5</i>	ACCCAGAGTTCATTGGATGCTG	AGCGCCTCTCTCTCCTTTGAAG
<i>WNT5A</i>	TTGAAGCCAATTCTTGGTGGTC	TGCAGAGAGGCTGTGCTCCTAT
<i>RHOQ</i>	TCTTCGACCACTACGCAGTCA	GGCCTCAGACGGTCATAGTCTT
<i>RKHD2</i>	GCCGCCAGGGTTGTAAAT	TTCACCACGAACAGGAGTCTT
<i>SLC7A11</i>	CGCCTTTTCAGGAAGAGATTCA	GGTAAAACCAGCCAGCATATGC
<i>ARFGEF1</i>	CTGCAGCACAGAGAGATGCG	AAAAGCGGTACATTCCCTTGGTC
<i>FBXO11</i>	GTGATGGACGAGGCCTTATTG	TGCACATAAATCCCACCATGC
<i>PTEN</i>	TCAGTGGCGGAACCTTGCAAT	GAACCTGTCTTCCCGTCGTGTG
<i>EZH2</i>	TGTCTTACTTGTGGAGCCGCT	TGGTGCCAGCAATAGATGCTT
<i>ACSL3</i>	GAGAGTTTGAACCCGATGGATG	CCAAGAGAAACATATTCCCCTGC
<i>HMGA2</i>	GAAGCAGCAGCAAGAACCAAC	GGACTCTTGTTTTTGCTGCCTT
<i>SLC6A15</i>	CTGGCCCAAGTTGGATTTTCT	TGGTAAAAGATATGCACCGCC
<i>SACS</i>	TTTGTCCCCTTCTCCTCATCT	CTTTAAAGCAGCCACAAGGTG
<i>FAM120A</i>	AACAAAGGCAGAAGGCTCGTC	ATGTCCATGTGGTTCCTGGTG
<i>MITF</i>	AAATGATCCAGACATGCGCTG	TTTGCGCGTTGCTGTTCTC
<i>SOX17</i>	GCATGACTCCGGTGTGAATCTC	AGTAATATACCGCGGAGCTGGC
<i>DRAM</i>	CTTGGTGCAGCCACGATGTAT	GGAGTGCTGAAATAGCAGTTTTG
<i>NLK</i>	TTCAGGCACAGAGTCCCATT	GCTGTTTATGAGGACCCCTGAG
<i>KPNA6</i>	TCCGGAAACTGCTCTCAAAG	ACCGATCCACCACTCTTGGAGT
<i>IPPK</i>	AGGATGCCAGCTCTGATCAAAG	CACAGACACGGAAAAGGCAAA
<i>INHBB</i>	ATCAGCTTCGCCGAGACAGAT	ACAGGTTCTGGTTGCCTTCGT
<i>CCNJL</i>	TCCTGCTTGCAAACGGAGTTT	GCAATGAGCTGAGATCATGCC
<i>ELAVL3</i>	GACCCCAATGATGCAGACAAA	GGTCTGGCATAGGACACCTTGA
<i>GGA3</i>	TGGAATCGATCAAGCCTAGCAG	CCTTGGCAAAGTGGAAAGAGGA
<i>TTN</i>	TGGAAGAGCTACTTCGACTGC	CGGGTTTGTCTTGATTCTGAG
<i>MKNK2</i>	CCTGGGCGTCATCTTGATATC	CTCCTGGATGCTCTCAAACAG
<i>ULK1</i>	AATGGATATAGCTCCGGCAGGA	AGCCTTGGAACCTTGCTGCTGTA

<i>AMOT</i>	AGCTCTAGAAGCTCGCATCCA	GGTCTTAATCCTGCCCTCCAT
<i>HELZ</i>	GAAGCAGCCAGCACACAAAGA	ACGTTCCACCACTTCAAACACC
<i>ARPP-21</i>	CAAGGAACTCCGGTGCAAAG	CTGGGTCATTGGCACCTGATA
<i>ANKS1B</i>	CTGCCTTTGATGTGAATTTAGCC	CTGGTAAGCGACTTCGAATGC
<i>HTR1B</i>	TGGTTATGCTATTGGCGCTCAT	CGGTACACTGTGGCAATCACAA
<i>ZDHHC6</i>	ACAGCTTTATCATCGGCTCTCC	ATTGGAAGAGGATCTCTCCGG
<i>FA2H</i>	ACTGTCTGGTACAGTGTCCCCA	GCAAAGGTTCCGGTAGTAGGACC
<i>IL6</i>	TCAATGAGGAGACTTGCCTGGT	CAGCTCTGGCTTGTTCTCTACT
<i>SEMA4G</i>	GCTTCACAGGCCTCATCATTGA	TGTCAGGAATGCTCCGGAATT
<i>ZBTB5</i>	GGAGCACATGAGAGTGGTGGTT	CACATCGCTCACTTCATCCTGA
<i>PARP6</i>	TTTCACCCATCCCCAAGTCTC	AGATGGAACGGTTCATGAGGC
<i>SCYL3</i>	TCCAGAATTCACAACTCTCCCA	GAGAACATCCGCTGAAACCTG
<i>LIMD2</i>	TCCACAACCTTTGCTTCTGCT	TTAAACAGCTGCTGGAAGTGG
<i>ATP6V0C</i>	TGGTCATGGCTGGCATCAT	TGGAGGAAGCTCTTGATAGAGGC
<i>SGSH</i>	TGACCGGCCTTTCTTCTCTA	GCTCTCTCCGTTGCCAACTT
<i>GALNS</i>	TTGTCGGCAAGTGGCATCT	CCAAACCACTCATCAAATCCG
<i>CTSA</i>	CAGGCTTTGGTCTTCTCTCCA	TCACGCATTCCAGGTCTTTG
<i>LRIG1</i>	AACCACGATAGAATGCTGACGG	GGAAGAATCCCCTTTCCCATC
<i>ARSA</i>	AGAGCTTTGCAGAGCGTTCAG	ATACGCATGGTCTCAGGTCCA
<i>SMAD2</i>	GAGACACCAGTTTTGCCTCCAG	TCCAGAGGCGGAAGTTCTGTT
<i>ZMYM6</i>	CTATAGTAGCTCTGGTCCTTGCCAA	TTCTGCTTGTATGCCGTGACA
<i>GNS</i>	CCCATTTTGGAGAGGTGCCAGT	TGACGTTACGGCCTTCTCCTT
<i>ZFYVE26</i>	CAGAAGATTCTGGGTTTGCAG	CATGACAGTTGATGGGTCTC
<i>LAMP1</i>	ACGTTACAGCGTCCAGCTCAT	TCTTTGGAGCTCGCATTGG
<i>UBXD2</i>	TGGTACTGTTGCCAGCAGGAA	ACAAGGTCCAAATGTCTCCGC
<i>BZW1</i>	ACCGTCGATATGCAGAAACAC	GCAAACACGCAGACATCTGTA
<i>SNAP23</i>	ATGGCCCTGAACATAGGCAAT	TGGTGTGAGCCTTGTCTGTGAT
<i>IQGAP1</i>	ACACCCACACTCTCCTGTTGGA	CAGTTCGTGGATTGGATCATTG
<i>GALNT2</i>	CTCAGCTGCAAGCCTTTCAA	TCCTGATGGTCTGGAACCCTT
<i>GABPA</i>	AGCCAAAGTACAAAGAGCGCC	TGGCCATTGTTTCTGTTCTG

Table S5. List of primer used to validate HOCTAR ranked list hsa-mir-98

Genes	Forward	Reverse
<i>HPRT1</i>	TGGACAGGACTGAACGTCTTGC	TTATAGCCCCCTTGAGCACA
<i>GAPDH</i>	ACTTCAACAGCGACACCCACT	GCCAAATTCGTTGTCATACCAG
<i>SNAP23</i>	ATGGCCCTGAACATAGGCAAT	TGGTGTGAGCCTTGTCTGTGAT
<i>ARMC8</i>	CCCTGCCTTATTGCAAGGACT	TGAAGATGGTACGCAGGCATC
<i>ATP2B1</i>	G TTCAGATTGGCAAAGCAGGTC	TGAACCCAGAAGGTGTCAATGA
<i>NRAS</i>	AACCTCAGCCAAGACCAGACAG	CAACCCTGAGTCCCATCATCA
<i>MAPK6</i>	GACATGACTGAGCCACACAAA	CTTCTGCTGTTAACCGATCCA
<i>C6orf211</i>	ACTCACCGTGGTTGTTGGTAGA	TGCATTGGTGGACTCTGGATAA
<i>HMGA2</i>	GAAGCAGCAGCAAGAACCAAC	GGACTCTTGTTTTTGTGCCTT
<i>UGCGL1</i>	GTTTGGCAGTTGCAAGATCTCAG	CATGACAACCAAAGCCAACTCA
<i>NRBF2</i>	AAGTAATGGAAGGACCCCTCA	CAGCTTCATGGCTTCAGAAAG
<i>RIOK3</i>	AGCTGGCCAAAGAATTGCAGT	TGGTCCTTCAGCAACAGCAAC
<i>IQGAP1</i>	ACACCCACACTCTCCTGTTGGA	CAGTTCGTGGATTGGATCATTG
<i>RAB8B</i>	CACCACCTTCATCTCCACCATC	CGCTGTGTCCCATATCTGAAGC
<i>THOC2</i>	TCAAACAACGACCGTGAAGTG	TGAAACCCCCATTGTTCCAT
<i>SMAD2</i>	GAGACACCAGTTTTGCCTCCAG	TCCAGAGGCGGAAGTTCTGTT
<i>EIF4G2</i>	AGTACTTTGCCCGAATGTGCTC	TACGGTATCCTGCAGCAGGAA
<i>EZH2</i>	TGTCTTACTTGTGGAGCCGCT	TGGTGCCAGCAATAGATGCTT
<i>EIF3S1</i>	T TCACTGACTGTGCTTTGCAG	GCCAGATCATCTTTCATGGTG
<i>BZW1</i>	ACCGTCGATATGCAGAAACAC	GCAAACACGCAGACATCTGTA
<i>LRIG1</i>	AACCACGATAGAATGCTGACGG	GGAAGAATCCCCTTTCCCATC
<i>NLK</i>	TTCAGGCACAGAGTCCCATTC	GCTGTTTATGAGGACCCCTGAG
<i>STAT3</i>	GTCAGGTTGCTGGTCAAATTCC	CAACGTCCCCAGAGTCTTTGTC
<i>POGZ</i>	TGCAGAATGCCAATCATGTGAC	TCCTTACAGGAAATCCCTGCG
<i>ULK2</i>	ATGGATATAGCTCCGGCAGGA	AGCCTTGGAAGTTGCTGCTGTA
<i>GALNT2</i>	CTCAGCTGCAAGCCTTTCAA	TCCTGATGGTCTGGAACCCTT
<i>TBC1D13</i>	CTGGCATCGCTTATGTGCAAG	GGCGTGCTCTTTCCACTCACTA
<i>SCYL3</i>	TCCAGAATTCACAACCTCTCCCA	GAGAACATCCGCTGAAACCTG
<i>ISL1</i>	TGGACGAGAGCTGTACATGCTT	CATTTGATCCCGTACAACCTGA
<i>PAK1</i>	ATTGGACAAGGTGCTTCAGGC	TGCTTAATGGCCACCTCCTGT
<i>ZBTB5</i>	GGAGCACATGAGAGTGGTGGTT	CACATCGCTCACTTCATCCTGA
<i>E2F6</i>	GCAGTTAAAGCTCCAGCAGAA	CCTGCTCCACTTCACACAAAT
<i>CDH22</i>	TTTCCCGCAGAAGATGTACCA	TTCTCTCCACGTCTGAGTCCT
<i>SFRS8</i>	CATGAAAGAGGGACGCTACAC	GCAAAGAGAGAGGGATGAAGG
<i>GABPA</i>	AGCCAAAGTACAAAGAGCGCC	TGGCCATTGTTTCCTGTTCTG
<i>SEMA4G</i>	GCTTCACAGGCCTCATCATTGA	TGTCAGGAATGCTCCGGAATT
<i>SEMA3F</i>	TGTCTTTACCTCCTCTGGCTCC	CCATGCGAATATCAGCCATG
<i>CPEB3</i>	AGCCTTTGGACCCAGAAAA	TGCCAGTTCAACAGCTCGAAG
<i>USP47</i>	CGCTGCTACAATGATTTGCGT	CTCGGAGCTTTCAACAAACACC
<i>PARP6</i>	TTTCACCCATCCCCAAGTCTC	AGATGGAACGGTTCATGAGGC
<i>EPHA4</i>	CAAGATACAGTGTGGCACTGGC	GCTTCGCTCATTCTGATCCTTC
<i>ZFYVE26</i>	CAGAAGATTCTGGGTTTGCAG	CATGACAGTTGATGGGTCCTC
<i>ADRB1</i>	TGCATCATGGCCTTCGTGTAC	CGCAGCTGTGATCTTCTTCA
<i>ODZ2</i>	GAGTCCGTTTCAAGCTTCAGGACA	AGGTCTTGAAGAGGAAGTGCCG
<i>ZNF248</i>	TCCAGGAACAAGTGTCAATTC	AATCTTCTGAGCAGGGTCCAG
<i>TTN</i>	TGGAAGAGCTACTTCGACTGC	CGGGTTTGTCTTGATTCTGAG
<i>LRRC3</i>	AAGCCTCTGGTTCAGGCTCT	GCGCACATAGTACACGACGTA

<i>ONECUT2</i>	ATGTGGAAGTGGCTTCAGGAG	GGGACTTCTTCTGGGAATTGT
<i>LIMD2</i>	TCCACAACCTCTTGCTTCTGCT	TAAACAGCTGCTGGAAGTGG
<i>ACSL3</i>	GAGAGTTTGAACCCGATGGATG	CCAAGAGAAACATATCCCCTGC
<i>ALDH5A1</i>	TATTTGACAGTGCCAACGTGG	TGAGCAAACACAAGTCTGTCCA
<i>ARSA</i>	AGAGCTTTGCAGAGCGTTCAG	ATACGCATGGTCTCAGGTCCA
<i>CHORDC1</i>	ATGGCCTTGCTGTGCTACAAC	GACCAACCCTTTAATGCATCGT
<i>CTNND2</i>	CCAGGAAAGATGCCATGACAG	TGTGTTTGATGTCTTCAGCGG
<i>CTSA</i>	CAGGCTTTGGTCTTCTCTCCA	TCACGCATTCCAGGTCTTTG
<i>FBXO11</i>	GTGATGGACGAGGCCTTATTG	TGCACATAAATCCCACCATGC
<i>GMFB</i>	GGTGGTACTGGATGAGGAGCTT	GAATCGAGGTTGTCGTTCAGG
<i>HELZ</i>	GAAGCAGCCAGCACACAAAGA	ACGTTCCACCACTTCAAACACC
<i>MTDH</i>	CCTCTAAAACCCGTCCAAAACA	TCGGTAGAAGTAGCAGGTGGAA
<i>MTX2</i>	TGCTGTTGACTGCAGAGCTGT	CCTAGCATGAGTGATCTCCCCT
<i>PSAP</i>	GCCAACAGTGAAATCCCTTCC	TCAGTGGCATTGTCTTCAGC
<i>PTEN</i>	TCAGTGGCGGAACTTGCAAT	GAACTTGTCTTCCCGTCGTGTG
<i>RCN2</i>	TTGATCCCCAAGAGCTGTTACC	CAATTAGATGAAGCGCCTCCTC
<i>RHOQ</i>	TCTTCGACCACTACGCAGTCA	GGCCTCAGACGGTCATAGTCTT
<i>SERBP1</i>	TCAAAGAGTGAAGAGGCTCATGC	GGTCTCCAAAATTGATCTCCAGC
<i>SGSH</i>	TGACCGGCCTTTCTTCTCTA	GCTCTCTCCGTTGCCAACTT
<i>UBE2A</i>	TGGACATACTCAGAACCGTTG	ATTGGGTTTCATCCAACAGAGAC
<i>ZMYM6</i>	CTATAGTAGCTCTGGTCCTTGCCAA	TTCTGCTTGTATGCCGTGACA

Table S6. List of primers used to validate Luciferase Assay

Genes	Forward	Reverse
<i>hsa-miR-26b</i>	AGGCTCTTCCCACCAATCC	GGCAGAGGCGCACAGGAAG
<i>hsa-miR-98</i>	GTCTTCTGCCTCCCTACACCTG	TCTGCCTCACCCTAAACACCA
<i>MAPK6</i>	CACTCAGCAGACATTTATCTTTGT	TGCTGGCCATGTTTTATTTG
<i>MTDH</i>	AAAACAAAACCTGCGGACACC	TGCCATGTTCTGAAACAGA
<i>RNF6</i>	GAGTATTTGGCTGAATGTTTGC	TTCGTTTTGTTTTCACTGGAGA
<i>CTSA</i>	CTCTCCCGCTAGGAGAGTCC	TCCTGAGCTCTGTTGGGTTT
<i>SNAP23</i>	TCCGTAGCTCCTCCTTGAAA	GGATCAAGCAGTGGTTATTGG
<i>ARMC8</i>	GCATCCCACCTCCTTGTTTA	GGGTGCAGAAAGGCTAACAG
<i>LRIG1</i>	GGGTTCAAGCGTCACTCATC	AAGACACTTCAATGCCATTTGT
<i>C6orf211</i>	CACCTTTTCATCCCCAGAAA	TGCAACAAAACATTTCCAGA
<i>POGZ</i>	TTAGGGAAAAGGGGGCATAC	AAGACAACCTTCTGGCCAAA